Inorganic Chemistry

Article

pubs.acs.org/IC

Rates of Water Exchange on the $[Fe_4(OH)_2(hpdta)_2(H_2O)_4]^0$ Molecule and Its Implications for Geochemistry

Adele F. Panasci,[†,‡] C. André Ohlin,[†,‡,§] Stephen J. Harley,[†,‡,∥] and William H. Casey*[,†,‡]

[†]Department of Chemistry and [‡]Department of Geology, University of California—Davis, 1 Shields Avenue, Davis, California 95618, United States

[§]School of Chemistry, Monash University, Victoria, 3800 Australia

[∥]Physical and Life Sciences Directorate, Lawrence Livermore National Laboratory, 7000 East Avenue, Livermore, California 94550-9698, United States

Supporting Information

ABSTRACT: The ammonium salt of $[Fe_4O(OH)(hpdta)_2(H_2O)_4]^-$ is soluble and makes a monospecific solution of $[Fe_4(OH)_2(hpdta)_2(H_2O)_4]^0(aq)$ in acidic solutions (hpdta = 2-hydroxypropane-1,3-diamino-*N*,*N*,*N*′,*N*′-tetraacetate). This tetramer is a diprotic acid with pK_{a1} estimated at 5.7 ± 0.2 and pK_{a2} = 8.8(5) ± 0.2. In the pH region below pK_{a1}, the molecule is stable in solution and ^{17}O NMR line widths can be interpreted using the Swift−Connick equations to acquire rates of ligand substitution at the four isolated bound water sites. Averaging five measurements at pH < 5, where contribution from the less-reactive conjugate base are minimal, we estimate: k_{ex}^{298} = 8.1 (±2.6) × 10^5 s^{-1}, $\Delta H^{\ddagger}$ = 46 (±4.6) kJ mol^{-1}, $\Delta S^{\ddagger}$ = 22 (±18) J mol^{-1} K^{-1}, and $\Delta V^{\ddagger}$ = +1.85 (±0.2) cm^3 mol^{-1} for waters bound to the fully protonated, neutral molecule. Regressing the experimental rate coefficients versus $1/[H^+]$ to account for the small pH variation in rate yields a similar value of k_{ex}^{298} = 8.3 (±0.8) × 10^5 s^{-1}. These rates are ∼10^4 times faster than those of the $[Fe(OH_2)_6]^{3+}$ ion (k_{ex}^{298} = 1.6 × 10^2 s^{-1}) but are about an order of magnitude slower than other studied aminocarboxylate complexes, although these complexes have seven-coordinated Fe(III), not six as in the $[Fe_4(OH)_2(hpdta)_2(H_2O)_4]^0(aq)$ molecule. As pH approaches pK_{a1}, the rates decrease and a compensatory relation is evident between the experimental $\Delta H^{\ddagger}$ and $\Delta S^{\ddagger}$ values. Such variation cannot be caused by enthalpy from the deprotonation reaction and is not well understood. A correlation between $\langle Fe^{III}-OH_2\rangle$ bond lengths and the logarithm of k_{ex}^{298} is geochemically important because it could be used to estimate rate coefficients for geochemical materials for which only DFT calculations are possible. This molecule is the only neutral, oxo-bridged Fe(III) multimer for which rate data are available.

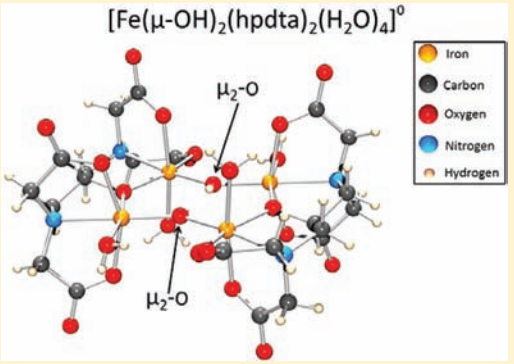

INTRODUCTION

Soil eliminates harmful contaminants from water and this purifying action originates largely from ligand- and electron-exchange reactions at the surface of iron-hydroxide and manganese-oxide minerals. In aerobic environments, the iron minerals have high-spin ferric irons separated by oxo- or hydroxo-bridges; these include goethite (α-FeOOH), hematite (α-Fe_2O_3), and lepidocrocite (γ-FeOOH). The minerals adsorb contaminant ions via ligand exchange at their surfaces, sometimes transforming them, and thus prevent the toxicants from entering drinking water and the biosphere. The reversal of these reactions can be profoundly dangerous − reductive dissolution of arsenic-rich ferric-hydroxide minerals, for example, may be the cause of mass arsenic poisonings in south Asia[5] where tens of millions of people are suffering from arsenic-related conditions. In this case, arsenic is released to groundwater when the ferric-hydroxide surface is reduced and the solid corrodes. This water is used for drinking.

Environmental scientists would like to be able to know and predict rates of ligand- and electron-exchanges at the functional groups on these mineral surfaces. This work is challenging because the surface structures are not well-known nor easily characterized. No spectrometric methods are yet able to easily measure the ligand-exchange rates in situ and predictions often rely heavily on computer simulations (refs 6 and 7). Ideally, these simulations would be tested using experiments on small oxide-bridged molecules for which the solution structures are confidently known and for which spectroscopic characterization is easy. Yet, there are surprisingly few experimental data describing elementary water-exchange reactions on Fe(III) complexes and virtually all of these are on monomeric complexes. Data exist for the $[Fe(H_2O)_6]^{3+}$ ion, the first hydrolysis complex, $[FeOH(H_2O)_5]^{2+}$,[3,8] and for aminocarboxylate monomer ions,[4,10] but most of these have seven-coordinated Fe(III) (Table 1). Rate information also exists for a small set of Fe(III)−porphyrin complexes that have six-coordinated Fe(III)[9,10] and two axially opposed bound waters.

Received: February 18, 2012
Published: June 6, 2012

   dx.doi.org/10.1021/ic300370q | *Inorg. Chem.* 2012, 51, 6731−6738

Table 1. Rate Data for Exchange of Bound and Bulk Waters for Various Aqueous Iron Complexes (Refs 29 and 30)[a]

complex	k^{298}	$\Delta H^{\ddagger}$	$\Delta S^{\ddagger}$	$\Delta V^{\ddagger}$	ref
		Fe(II)			
$[Fe(H_2O)_6]^{2+}$	4.39×10^6	41.4	+21.2	+3.8	35
$[Fe(EDTA)(H_2O)]^{2-}$	2.7×10^6	43.2	+23	+8.6	36
		Fe(III)			
$[Fe(H_2O)_6]^{3+}$	1.6×10^2	64.0	+12.1	−5.4	3
$[Fe(OH_2)OH]^{2+}$	1.2×10^5	42.4	+5.3	+7.0	3, 9, 27
$[Fe(CDTA)(H_2O)]^{-}$	1.3×10^7	27	−18	+4.0	34
$[Fe(EDTA)(H_2O)]^{-}$	7.2×10^7	24.3	−13	+2.2	34
$[Fe(HEDTA)(H_2O)]^{0}$	7.8×10^7	22	−20	+2.1	34
$[Fe(EDDS)(H_2O)]^{-}$	4.3×10^5	48	+24	−14.4	34
$[Fe(PhDTA)(H_2O)]^{-}$	1.2×10^7	26	−22	+4.6	4
$[Fe(\alpha\text{-EDDADP})(H_2O)]^{-b}$	2.3×10^8	36	+36	+3.0	34
	2.5×10^6	24	−42		
$[Fe(TPPS)(H_2O)_2]^{3-}$	2.0×10^6	67	+99	+7.9	9
	1.4×10^7	57.3	+84.5		10
$[Fe(TMPyP)(H_2O)_2]^{5+}$	4.5×10^5	71	+100	+7.4	9
	7.8×10^5	57.7	+67.5		10
$[Fe(TMPS)(H_2O)_2]^{3-}$	2.1×10^7	61	+100	+11.9	9
$[Fe_4(OH)_2(hpdta)(H_2O)_4]^{0}$	8.1×10^5	46	+22	+1.85	this paper
$Mo_{72}Fe_{30}$[b]	6.7×10^6	26.3	−26		1

[a] CDTA = cyclohexanediaminetetraacetic acid; EDTA = ethylenediaminetetraacetate, CDTA = *trans*-1,2-diaminocyclohexanetetraacetate, HEDTA = monoprotonated form of EDTA, EDDS = *s,s*-ethylenediaminedisuccinate, PhDTA = *o*-phenylenediamine-*N,N,N′,N′*-tetraacetato, EDDADP = ethylenediaminediacetatedipropionate, H_2TPPS = *meso*-tetrakis(*p*-sulfonateophynyl)prophine, H_2TMPyP = *meso*-tetrakis(*N*-methyl-4-pyridyl)porphine, H_2TMPS = *meso*-tetrakis-(sulfonatomesityl)porphine. [b] Stoichiometry for this molecule is: $[Mo_{72}Fe_{30}O_{252}(CH_3COO)_{12}[Mo_2O_7(H_2O)]_2[H_2Mo_2O_8(H_2O)](H_2O)_{91}]\cdot\sim 150H_2O$.

Data on multimeric Fe(III) molecules with oxide bridges and isolated waters would, of course, be most relevant to geochemistry because these can be used to better approximate the oxo- and hydroxo-bridged surface metals. However, save for the data of Balogh et al.[1] on a Keplerate ion, there are no measurements for water-exchange rates on multinuclear iron complexes (Table 1).

In this article, we describe water-exchange rates for a tetra-Fe(III) molecule, which has both a μ_3-oxo bridging two Fe(III) and a carbon, and a μ_2-OH bridge in the inner-coordination sphere of each of the four Fe(III) centers. This molecule is one of a class of potential molecular magnets[11−16] and we selected the $[Fe_4(OH)_2(hpdta)_2(H_2O)_4]^0$(aq) molecule (hpdta = 2-hydroxypropane-1,3-diamino-*N,N,N′,N′*-tetraacetate) for detailed study among these multinuclear complexes because of its aqueous stability and solubility. In solution, this molecule presents an isolated Fe-bound water in a well-constrained structure and adjacent to oxo bridges. This molecule has two sets of iron-bound bridging oxygens in the inner-coordination sphere of each of the four Fe(III) (Figure 1) and the bound waters are isolated from one another.[17] Our ultimate goal is to establish a firm correlation between experimental rates of water exchange with some simple easily calculable or measurable property, such as $\langle Fe^{III}-OH_2\rangle$ bond lengths. New experimental developments, such as crystal-truncation-rod X-ray-scattering experiments,[18] indicate that $\langle Fe^{III}-OH_2\rangle$ bond lengths may be soon measurable at the aqueous−mineral interface and they can certainly be calculated using ab initio methods. Thus, such a correlation for high-spin oxo Fe(III) complexes would be a useful advance.

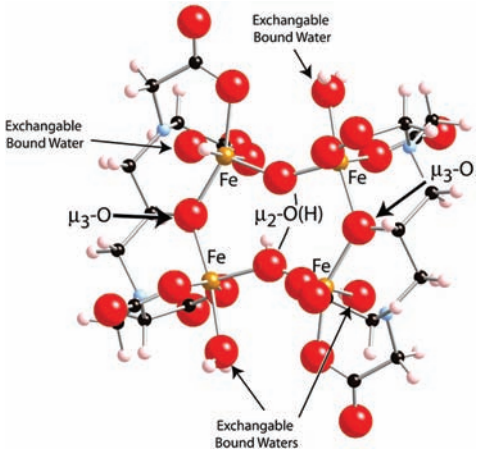

Figure 1. $[Fe_4O(OH)(hpdta)_2(H_2O)_4]^-$ ion in crystals of $[Fe_4O(OH)(hpdta)_2(H_2O)_4](NH_4)\cdot 9H_2O$.[2] The site labeled μ_2-O(H) indicates a proton disordered between the two equivalent μ_2-oxo bridges in the solid state. Both of these bridges are fully protonated at pH < pK_{a1} in solution. The inner-coordination sphere of each Fe(III) has a single bound water, one μ_2-OH bridge, one μ_3-oxo bridge, a bound amine nitrogen, and two carboxylate oxygens.

EXPERIMENTAL METHODS

Synthesis and Characterization. $[Fe_4O(OH)(hpdta)_2(H_2O)_4](NH_4)\cdot 9H_2O$ [**1**] (hpdta = 2-hydroxypropane-1,3-diamino-*N,N,N′,N′*-tetraacetate) was made according to Schmitt et al.[19] (Figure 1). NH_3(aq) (2 M, 84 mL) was added to an aqueous suspension of H_5hpdta (5.18 g, 64 mL). The resulting solution was added dropwise to a stirred solution of $Fe(NO_3)_3\cdot 9H_2O$(aq) (0.34 M, 80 mL) leading to a change in color from yellow to dark red. Dimethyl acetamide (64 mL) was added to the solution and slow evaporation over several days yielded brick-red platelike crystals with a yield of 37% based on $Fe(NO_3)_3\cdot 9H_2O$. The crystals were collected by filtration, air-dried, and ground to afford a homogeneous powder. Elemental analysis by Galbraith Laboratories of $C_{22}Fe_4H_{57}N_5O_{33}$ found (Calcd): C 22.8 (23.12), H 5.56 (5.03), N 8.42 (6.13), Fe 16.50 (19.54), O 46.72 (46.19) % w/w. The crystallographic cell parameters are consistent with those reported by Schmitt et al.[3]

Aqueous solutions of the compound at the self-buffering pH were characterized by ESI-MS at a cone voltage of −20 V using an HP Agilent MSD G1956b single-quadrupole electrospray-ionization mass spectrometer equipped with a syringe pump for direct injection of solutions into the spray chamber at 30 μL min^{-1}. Signals corresponding to $[Fe_4O(OH)(hpdta)_2]^-$ (890.9 *m/z*), $[Fe_4O_2(hpdta)_2]^{2-}$ (444.9 *m/z*), and $[Fe_4(hpdta)O_3]^{3-}$ (302.3 *m/z*) were observed. Assignments were confirmed by comparing the peak shapes with theoretical isotopic envelopes (Figure 2).

Solution Chemistry. Evidence for two pK_a values was found in the pH region 4 < pH < 8 both by acid−base potentiometry and by modeling UV−vis spectra as a function of pH. Potentiometric titrations were performed using a Metrohm 718 STAT Titrino autotitrator and a 5 mM solution of [**1**] with 0.1 M KNO_3 background salt. Titration was done by addition of 0.1 M KOH followed by back-titration using 0.1 M HNO_3. The titration over the region 4 < pH < 8 was reversible (Figure 3). Plots of uncompensated charge (*Z*) versus pH were consistent with a single protonation reaction when pH ∼ pK_{a1}:

dx.doi.org/10.1021/ic300370q | Inorg. Chem. 2012, 51, 6731−6738

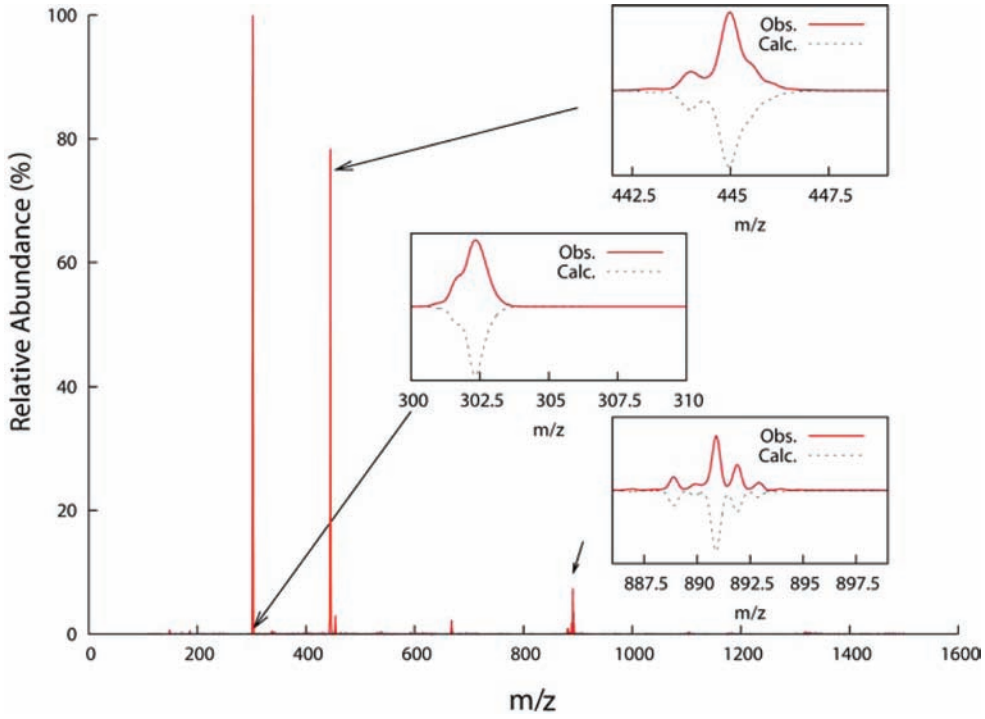

Figure 2. Plot of a negative-ion ESI-MS spectra of [**1**] taken at pH ~6 corresponding to the natural pH upon dissolution of the crystals into water. The three insert plots show the observed and calculated spectra for the most-abundant peaks: 302.3 m/z corresponding to $[Fe_4(hpdta)_2O_3]^{3-}$, 444.9 m/z corresponding to $[Fe_4(hpdta)_2O_2]^{2-}$, and 890.9 m/z corresponding to $[Fe_4(hpdta)_2O(OH)]^{-}$.

$$Z = \frac{[H^+] + [K^+] - [NO_3^-] - [OH^-]}{[Fe_4O(OH)(hpdta)_2(H_2O)_4]_{Total}} \quad (1)$$

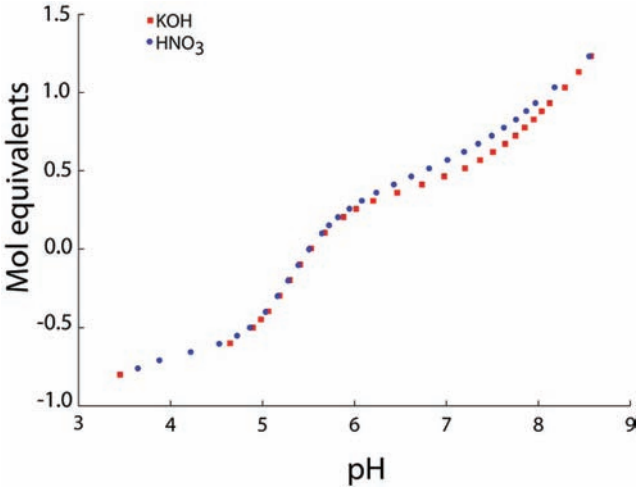

Figure 3. Titration of $[Fe_4O(OH)(hpdta)_2(H_2O)_4](NH_4)\cdot 9H_2O$ (5.04 mM, 5 mL volume) in 0.1 M KNO_3 using 0.100 M HNO_3 and 0.105 M KOH. See Supporting Information for data.

UV–vis titrations were carried out using a Cary 300 UV–vis spectrometer. Three mL samples of 0.222 mM $[Fe_4O(OH)(hpdta)_2(H_2O)_4](NH_4)\cdot 9H_2O$ with 13.1 mM $TMAClO_4$ (TMA = tetramethylammonium) background salt were made with varying amounts of $HClO_4$ and TMAOH to create a series of samples with pH values that ranged from 3.7 to 10.2. For each sample, the absorbance for $200 < \lambda < 800$ nm was recorded.

NMR Spectroscopy. Nuclear magnetic resonance (NMR) measurements were carried out on the solutions using a Bruker Avance DRX 500 MHz (11.75 T, ^{17}O:67.8 MHz; ^{31}P:202.4 MHz) spectrometer equipped with a 5 mm broad-band probe. The ^{17}O spectra were acquired using single-pulse excitations using 10.5 μs $\pi/2$ pulses with 0.6 s recycle delay. The sweep width was set to 2042.48 Hz. The samples were also enriched in ^{17}O; to a 3 ml sample was added 10 μL of 40% $H_2{}^{17}O$ (Isotec Laboratories) so that eight acquisitions could establish adequate signal-to-noise ratio in the spectrum. Temperature was controlled using the Bruker Avance system temperature controller, which is precise and accurate to ±0.5 °C. An acidified 0.05 M $NaClO_4$ solution was used as the diamagnetic standard.

Rate experiments were initiated by dissolving varying amounts, but typically 0.012 g, of [**1**] in 463 μL of 0.108 M sodium perchlorate solution. Microliter amounts of perchloric acid were added to lower the pH and then the solutions were brought up to a volume of 1.00 mL. In these experiments, the final $[Fe_4O(OH)(hpdta)_2(H_2O)_4](NH_4)\cdot 9H_2O$ concentration was 10 mM and the sodium perchlorate concentration was 0.05 M. Although the molecule is persistent for days in the pH range $4.0 < pH < 8.5$, and detectable as an intact molecule in ESI-MS spectra, it dissociates in strongly acidic solutions to form Fe(III) monomers and ultimately iron-hydroxide colloids. At pH > 9, there is evidence for some irreversible change in structure, such as formation of higher-nuclear complexes, as has been suspected.[20]

High-pressure NMR experiments were performed in a wide-bore Bruker Avance 400 MHz (9.4 T) spectrometer using a home-built high-pressure probe[21] similar to that used in previous experiments.[22−24] The sample was sealed in a custom high-pressure quartz NMR tube with a dual Viton O-ring plunger and the probe pressure was set with a high-pressure syringe pump in combination with a valve system. *iso*-Hexane was used as the pressure-conduit fluid; pressures were continuously monitored and never allowed to fluctuate more than 0.5% during data acquisition. The temperature was kept constant via a circulating water bath and was monitored with a type-T thermocouple situated in the probe body near the probe head and at pressure. Thermal equilibrium was established after each pressure increase before data were acquired. We used a calibrated 45 μs $\pi/2$ pulse with a 0.4 s relaxation delay.

Rates were estimated via a Swift–Connick formalism.[22,23] Briefly, a two-site exchange mechanism in the dilute-solution limit allows for the

dx.doi.org/10.1021/ic300370q | *Inorg. Chem.* 2012, 51, 6731−6738

peak widths to be interpreted using a simplified form of the steady-state Bloch–McConnell equations (ref 23). The experimental line widths are first adjusted for the presence of the diamagnetic standard: $1/T_{2r} = (\pi/P_m)(\Delta\nu_{obs} - \Delta\nu_{solvent})$. The equation:

$$\frac{1}{T_{2r}} = \frac{1}{\tau_m}\left[\frac{T_{2m}^{-2} + (T_{2m}\tau_m)^{-1} + \Delta\omega_m^2}{(T_{2m}^{-1} + \tau_m^{-1})^2 + \Delta\omega_m^2}\right] \quad (2)$$

is derived from Swift–Connick line-broadening analysis (refs 22 and 23) where P_m is the mole fraction of bound waters (here four) divided by the mole fraction of solvent water and τ_m is the exchange time, which relates directly to the rate coefficient, $\tau_m = 1/k_{ex}$. The temperature variation of the exchange time was described using the Eyring–Polanyi equation: $1/\tau_m = (k_B T/h)\exp(\Delta S^{\ddagger}/R - \Delta H^{\ddagger}/RT)$. The temperature variations of $1/T_{2m}$ is exponential with $1/T$ and $\Delta\omega_m$ is linear with the inverse temperature (description in Harley et al.[23]). The result was a system of nonlinear equations in $1/T_{2r}$ that could be minimized using a Levenberg–Marquardt algorithm with data collected over a wide range of temperatures and P_m values. The

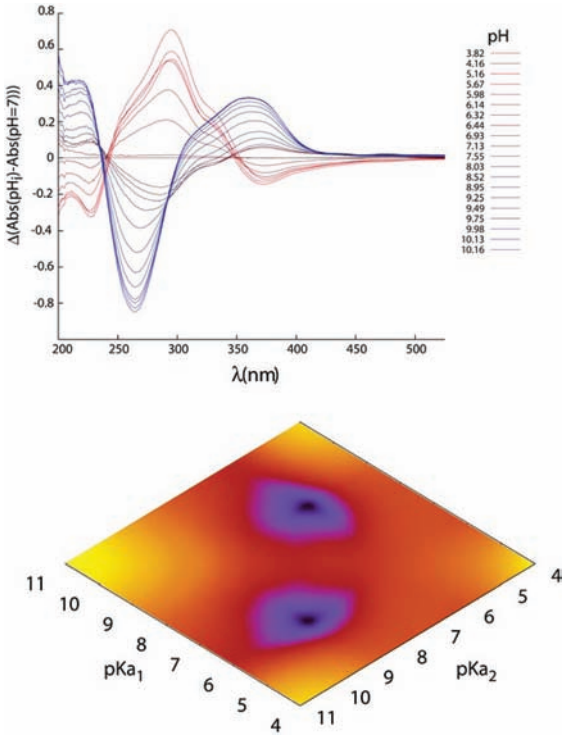

Figure 4. (Top) UV–vis difference spectra of [**1**] as a function of solution pH. The difference spectra were calculated by subtracting the absorbance at a given wavelength at pH 6.44 from that of the absorbance at a given pH at the same wavelength. Two isosbestic points are evident and interpreted to indicate protonation of the complex. (Bottom) Least-squares fitting of the UV–vis titrations detected two significant pK_a values at pK_{a1} = 5.9 (±0.1) and pK_{a2} = 8.8 (±0.1). Plotted is the variable $\ln[((\Sigma_1(\text{Abs.}(\lambda_i)_{obs} - \text{Abs.}(\lambda_i)_{calcd})^2)/Z)]$ as a function of pK_{a1} and pK_{a2}, where Z is a scaling factor based on the maximum residual.

temperature variation of the experimental data (Figure 5) has enough curvature to require fitting $1/T_{2r}$ to a form of eq 2 that includes paramagnetic contributions to chemical-shift variations; these were used as adjustable parameters. Uncertainties are standard deviations calculated from the covariance matrix obtained from the regression (Table 2).

The pressure dependence of k_{ex} at a temperature where $T_{2m}^{-1} \gg \Delta\omega^2, \tau_m^{-1}$ yields the activation volume, $\Delta V^{\ddagger}$: $\ln[k(P)] = -(\Delta V^{\pm}/RT)P - \ln[k^{\circ}]$, where $k(P)$ is the pressure-dependent rate constant, P is

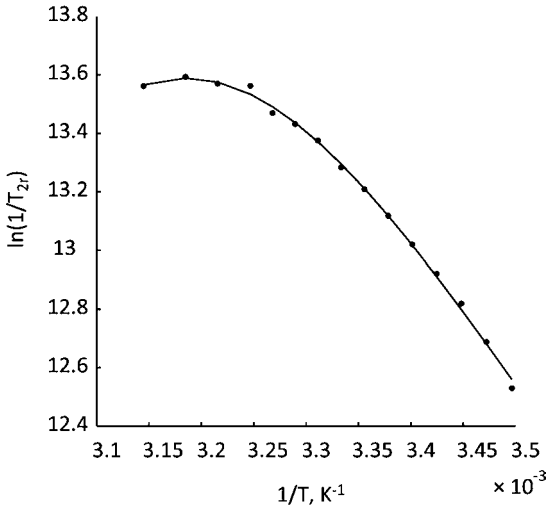

Figure 5. ^{17}O NMR line width information as a function of temperature for a 10 mM solution of the $[Fe_4(OH)_2(hpdta)_2(H_2O)_4]^0$(aq) molecule at pH 4.95. The line corresponds to the nonlinear fit obtained by minimizing a system of nonlinear equations using Levenberg–Marquardt algorithm. Minimized parameters were used to estimate rate coefficients for exchange of bound and bulk waters.

Table 2. Rate Parameters for Rates of Exchange of Waters Bound to [1] Derived from ^{17}O NMR Line Widths and Assuming That There Are Four Exchangeable Waters Bound to Each Molecule

pH	concentration (mM)	k^{298} (10^5 s^{-1})[a]	$\Delta H^{\ddagger}$ (kJ mol^{-1})[a]	$\Delta S^{\ddagger}$ (J mol^{-1} K^{-1})[a]
3.8	12.7	9.7 ± 1.2	49.2 ± 0.2	+34.6 ± 4.2
4.5	11.6	12.0 ± 3.0	52.7 ± 0.4	+48.3 ± 12
4.7	12.6	6.4 ± 1.5	43.4 ± 0.8	+11.8 ± 2.7
4.9	11.7	6.9 ± 3.0	42.9 ± 0.2	+10.8 ± 5.8
4.95	10.5	5.9 ± 1.8	42.3 ± 0.1	+7.8 ± 2.3
5.2	12.1	6.6 ± 6.5	38.6 ± 0.1	−4.0 ± 3.9
5.2	7.3	6.3 ± 1.9	34.4 ± 0.15	−18.4 ± 5.4
5.2	11.7	4.5 ± 3.0	36.5 ± 0.35	−14.2 ± 9.6
5.2	14.1	6.05 ± 1.1	37.8 ± 0.4	−7.4 ± 14
5.2	19.2	5.3 ± 1.4	36.0 ± 0.2	−14.5 ± 4
5.4	10.0	4.5 ± 1.8	34.2 ± 0.3	−22.3 ± 11
5.5	11.5	1.7 ± 0.1	25.0 ± 1.3	−60.9 ± 4.4
5.8	10.0	1.9 ± 0.2	18.9 ± 2.0	−80 ± 7

[a]Uncertainties in $\Delta H^{\ddagger}$ and $\Delta S^{\ddagger}$ are reported as single standard deviation in the regression. Uncertainties in values of k^{298} are also reported as the standard error of the regression, but this uncertainty is probably too small. A more conservative estimate of uncertainty is a factor of ~2 in k^{298} and can be estimated by propagating errors of $\Delta H^{\ddagger}$ and $\Delta S^{\ddagger}$ through $k(T) = (((k_B T)/h))\exp(((\Delta S^{\ddagger})/R) - ((\Delta H^{\ddagger})/RT))$ via Monte Carlo methods; the resulting uncertainty in $\log(k^{298})$ is ±0.3 or less.

pressure, R is the gas constant, k° is the pressure at near-ambient conditions, and T the temperature (Figure 6).

Magnetic Susceptibility Measurements. Magnetic susceptibility measurements of [**1**] were made using a Quantum Design SQUID Magnetometer MPMS-2 and obtained results identical to those of Schmitt et al.[15] and are included in the Supporting Information. Schmitt et al. studied the magnetism of [**1**] extensively and showed that the susceptibility increases with increasing temperature, which is typical behavior of an antiferromagnetic system with a ground state S = 0. The magnetic susceptibility of [**1**] did not reach a maximum in the

dx.doi.org/10.1021/ic300370q | Inorg. Chem. 2012, 51, 6731–6738

temperature range 5−300 K, so the Néel point could not be calculated (Supporting Information).

RESULTS

To be useful as a model, the molecule: (i) must remain intact at conditions of the NMR experiments, (ii) the protonation state must be known, and (iii) the rate parameters must be well-defined at the experimental pH. Three independent lines of evidence indicate that the molecule is stable in solution with the $[Fe_4(OH)_2(hpdta)_2(H_2O)_4]^0(aq)$ stoichiometry. First, the acid−base chemistry, as inferred from both the UV−vis data and the potentiometry, indicates that the molecule undergoes a reversible deprotonation near pH ∼5.7 (±0.2, below). Second, these data are consistent with the ESI-MS data, which indicate that the core of the molecule remains intact during analysis. Third, the ^{17}O NMR data indicate that rates vary slowly with pH at pH < 5 (Table 2), suggestive of a conjugate base with a different reactivity than the fully protonated $[Fe_4(OH)_2(hpdta)_2(H_2O)_4]^0(aq)$ molecule.

Figure 3 shows the acid base titration of [**1**] and Figure 4 shows the UV−vis titration data between 4 < pH < 10. There are two isosbestic points clearly evident in Figure 4 (top), consistent with the presence of two pK_a values in the pH range (Figure 4, bottom). We applied a numerical method to fit the spectra using a nonlinear least-squares analysis (ref 24) resulting in pK_{a1} and pK_{a2} values of 5.9 (±0.1) and 8.8 (±0.1) respectively, which compare well with the potentiometry. The potentiometry indicated two clear inflection points with: pK_{a1} = 5.5 (±0.15) and pK_{a2} = 8.9 (±0.2). Whereas the potentiometry could be affected by protonation of NH_3 near pK_{a2}, the UV−vis data are not and clearly indicate that these pK_a values correspond to protonation on the iron complex. We average these two values of pK_{a1} and assign pK_{a1} = 5.7 (±0.2), which we use for subsequent discussion. Potentiometric titrations as a function of temperature yielded the enthalpy of the first deprotonation reaction via the van't Hoff equation with ΔH_{rxn} = 63.3 (±5.9) kJ mol^{-1} (Supporting Information).

At pH < 3, the molecule dissociates and releases monomeric Fe(III) to solution, which is easily detectable in the UV−vis spectra and, over several days, ferric-hydroxide colloids could be detected in these acidic solutions by light-scattering methods. The potentiometry becomes irreversible if extended to pH > 9 indicating a change in structure beyond pK_{a2}.

The acidic protons are probably on the μ_2-oxo bridges and not on the bound waters. X-ray structure of the $[Fe_4O(OH)(hpdta)_2(H_2O)_4](NH_4)\cdot 9H_2O$ salt indicates a single proton disordered between the two μ_2-oxo bridges (Figure 1). Dissolution of this molecule into the degassed water results in a mildly acidic solution (pH ∼6) consistent with pK_{a1} = 5.7 (±0.2).

The most reasonable interpretation is that one of the μ_2-OH bridges deprotonates as solids precipitate at near-neutral pH making the ionic crystal. This result may be surprising given the strong acidity of waters in the $[Fe(H_2O)_6]^{3+}$ ion (pK_{a1} ∼2.4[25]) at this ionic strength, however, the hpdta molecule is an aminocarboxylate and withdraws enough charge from the metal centers to dramatically decrease the acidity of the bound waters to Fe(III) centers. The bound water in the Fe(III)−PhDTA complex (PhDTA = *o*-phenylenediamine-*N*,*N*,*N*′,*N*′,-tetraacetato), for example, dissociates at pH > 8 (pK_a = 8.71 (±0.02) at 298 K and I = 1.00 M $NaClO_4$[4]). In this case, the Fe(III) is coordinated to seven ligand atoms, not six as in our molecule [**1**], but the reduced acidity for Fe(III)-bound waters is consistent. The acid−base titration data for [**1**] are reproducible at pH < pK_{a1} where the complex has the stoichiometry $[Fe_4(OH)_2(hpdta)_2(H_2O)_4]^0(aq)$.

Averaging the data in Table 2 for pH < 5, we estimate: k_{ex}^{298} = 8.1 (±2.6) × 10^5 s^{-1}, $\Delta H^{\ddagger}$ = 46 (±4.6) kJ mol^{-1}, $\Delta S^{\ddagger}$ = 22 (±18) J mol^{-1} K^{-1} for the fully protonated, neutral molecule, $[Fe_4(OH)_2(hpdta)_2(H_2O)_4]^0(aq)$. The fraction of the conjugate base at pH < 5 is 17% or less. Supporting the assignment of these rate data to the fully protonated molecule is the well-known empirical relation between $\Delta H^{\ddagger}$ and $\ln(k_{ex}^{298})$ for water-exchange reactions (Figure 3 in ref 26 and Figure 5 in ref 27) and the values reported here for the $[Fe_4(OH)_2(hpdta)_2(H_2O)_4]^0(aq)$ ($\Delta H^{\ddagger}$ = 46 (±4.6) kJ mol^{-1} and k_{ex}^{298} = 8.1 (±2.6) × 10^5 s^{-1}) fall well on this correlation.

Causes of the compensatory pH variation of rate data, however, are unclear. The pH variation can be seen by regressing values of the observed rate coefficient as a function of 1/[H$^+$] [Figure 6, top] assuming that there are two pathways, with one corresponding to the fully protonated $[Fe_4(OH)_2(hpdta)_2(H_2O)_4]^0(aq)$ molecule, which reacts independent of pH, and a second assumed pathway that is proportional to the concentration of the conjugate base, $[Fe_4O(OH)(hpdta)_2(H_2O)_4]^{-1}(aq)$, and thus depends on pH. Assigning $k_{ex}^{298} = k_{obs}$, the empirical rate coefficients for two pathways can be resolved via a linear regression of: $k_{obs} = k_1 + K_{a1}k_2/[H^+]$. The linear-least-squares intercept is $k_1 = k_{ex}^{298}$ = 8.3 (±0.75) × 10^5 s^{-1}, close to the average of values at pH < 5, above.

We have no confidence in assigning rate coefficients to the conjugate base $[Fe_4O(OH)(hpdta)_2(H_2O)_4]^{-1}(aq)$ because of uncertainty in the regressed data. The regression slope in Figure 6 (top), −1.32 (±0.3), when multiplied by the estimate of K_{a1} (pK_{a1} = 5.7 (±0.2)), yields an estimate of k_2 = 2.6 (±0.6) × 10^5 s^{-1} for $[Fe_4O(OH)(hpdta)_2(H_2O)_4]^{-1}(aq)$ (Figure 6 (top)). This estimate of the rate coefficient unsurprisingly indicates a lower reactivity than for the fully protonated $[Fe_4(OH)_2(hpdta)_2(H_2O)_4]^0(aq)$ form.

The pressure dependencies of the reduced ^{17}O NMR linewidths were determined at two conditions (pH 4.6, 291 K; pH 5.1, 298 K) and the results are shown in Figure 6 (bottom). Values of $\Delta V^{\ddagger}$ were estimated by linear-least-squares fits of the pressure variation of the reduced linewidths and the resulting values were virtually indistinguishable: $\Delta V^{\ddagger}$ = 1.9 (±0.2) cm^3 mol^{-1} at pH 4.6 and $\Delta V^{\ddagger}$ = 1.8 (±0.2) cm^3 mol^{-1} at pH 5.1 indicating an exchange pathway that does not strongly depend on pH at these conditions.

DISCUSSION

The reactivity of bound waters in the $[Fe_4(OH)_2(hpdta)_2(H_2O)_4]^0(aq)$ molecule are broadly similar to those bound to other Fe(III)−aminocarboxylate ions and are more labile than waters in the $[Fe(H_2O)_6]^{3+}$ ion (Table 1) by a factor of ∼10^4 . To a first approximation, we interpret these differences in labilities to reflect changes in charge on the Fe(III) metal centers and thus should also correlate with bond lengths, although a more sophisticated view of electronic structure may ultimately be necessary.[28] The ⟨Fe^{III}−OH_2⟩ bond length in crystals of $[Fe_4O(OH)(hpdta)_2(H_2O)_4](NH_4)\cdot 9H_2O$, ⟨2.07 Å⟩, is considerably longer than that of $[Fe(H_2O)_6]^{3+}$, which is ⟨1.986 Å⟩.[2,29] We add these data to the figure of Balogh et al.[1] correlating reactivity with ⟨Fe^{III}−OH_2⟩ bond lengths (Figure 7).

dx.doi.org/10.1021/ic300370q | *Inorg. Chem.* 2012, 51, 6731−6738

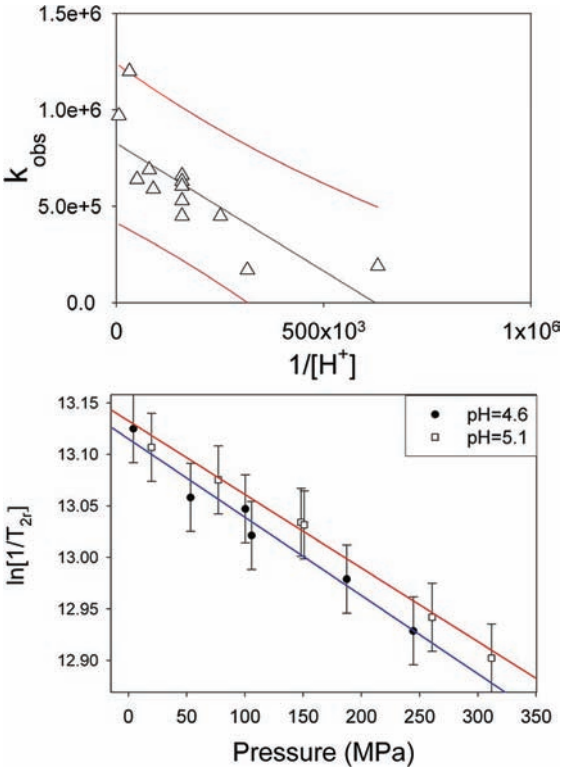

Figure 6. (Top) Regression of the average rate coefficient extracted from the experiments, here defined as k_{obs}, against $1/[H^+]$. The 95% prediction intervals are shown in red. (Bottom) ^{17}O NMR relaxation information yielding ligand-exchange rates for the $[Fe_4(OH)_2(hpdta)_2(H_2O)_4]^0(aq)$ molecule as a function of pressure. The filled circles indicate experiments conducted at 18 °C, pH 4.6 and a concentration of [**1**] of 15 mM. The red line corresponds to a linear regressions through the data to yield $\Delta V^{\ddagger}$ = 1.9 (±0.2) cm^3 mol^{-1}. The unfilled squares indicate data from experiments at pH 5.1 at 25 °C at 14 mM total concentration of [**1**]. The blue line indicates the regression that yields: $\Delta V^{\ddagger}$ = 1.8 (±0.1) cm^3 mol^{-1}. Uncertainties were estimated at ±4 Hz and were determined from replicated measurements.

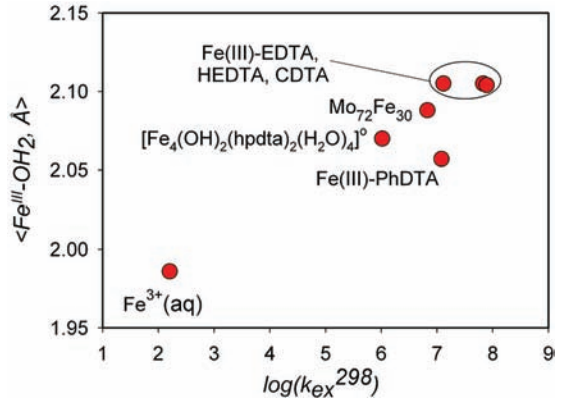

Figure 7. Correlation between the $\log(k_{ex}^{298})$ and the $\langle Fe^{III}-OH_2\rangle$ bond length in the corresponding solid. The EDTA and CDTA complexes are monoanionic, the HEDTA complex is neutral, and the EDTA, CDTA, and HEDTA complexes correspond to seven-coordinated, high-spin Fe(III). The data for the $Mo_{72}Fe_{30}$ is from Balogh et al.[1] and corresponds to >Fe−OH_2 functional groups exposed on a ∼1500 atom, nanometer-size Keplerate molecule. The value for the $[Fe_4(OH)_2(hpdta)_2(H_2O)_4]^0(aq)$ molecule is described in this article and has four hexacoordinated Fe(III) centers, an isolated bound water, and sets of μ_2-OH and three-coordinated oxo in the inner-coordination-sphere of each metal. The Fe(III)−PhDTA complex has a single bound water[4] and also has a seven-coordinated Fe(III) center.

The correlation (Figure 7) is sparse because there is a relatively small set of Fe(III) complexes where both bond lengths in the solid state and rate coefficients are known. Furthermore, among the data, the aminocarboxylate complexes have seven-coordinated iron. Also included in this cohort is a complex where one of the acetate groups on the [EDTA] ligand is protonated (indicated as HEDTA in Table 1) so that the complex has no net charge in solution. This datum shows that neutralization of charge on the molecule caused only a minor increase in lability of the bound water, from k_{ex}^{298} = 7.2 × 10^7 s^{-1} to 7.8 × 10^7 s^{-1}. Similarly, the Fe(III)−PhDTA complex is also a seven-coordinated aminocarboxylate with no net charge at the pH conditions where rates were measured.[4] Our data here for $[Fe_4(OH)_2(hpdta)_2(H_2O)_4]^0(aq)$ molecule is for a structure with six-coordinated iron that is neutral in solution.

The correlation shown in Figure 7 is also heavily influenced by two values. The value of k_{ex}^{298} = 160 s^{-1} is the smallest and experimentally best-constrained number, from multiple experiments.[3,8,30] The value assigned to functional groups on the large Keplerate molecule, labeled $Mo_{72}Fe_{30}$ are much less certain. Balogh et al.[1] derived the estimate from studies of ^{17}O NMR relaxation but, unlike all other data shown in Table 1, they found no clear area of activation similar to the data shown in Figure 5. They instead estimated the rate coefficients in a nonlinear least-squares analysis, in a manner analogous to work on gadolinium imaging agents.[31]

The activation volume for the iron complex $[Fe_4(OH)_2(hpdta)_2(H_2O)_4]^0(aq)$ is a small positive value ($\Delta V^{\ddagger}$ = +1.85 cm^3 mol^{-1}), also consistent with other values in large aminocarboxylate complexes (Table 1), and which indicates a dissociative interchange mechanism, $\mathbf{I_D}$, if interpreted using the traditional formalism derived for octahedral metal ions.[31,32] Within this formalism, the majority of the ferric iron complexes in Table 1 also would be classified as exhibiting $\mathbf{I_D}$ mechanism for water exchange meaning a slightly positive, but small, $\Delta V^{\ddagger}$ value. One interpretation is that donation of electron density to Fe(III) from nitrogens in the ligand leads to increased $\langle Fe^{III}-OH_2\rangle$ bond lengths that favor a dissociative exchange mechanism.[33] A simple example is in the octahedral hydrolysis complexes of Fe(III). For $[Fe(OH_2)_6]^{3+}$, k_{ex}^{298} = 160 s^{-1} and $\Delta V^{\ddagger}$ = −5.4 cm^3 mol^{-1}. Upon hydrolysis to form $[FeOH(OH_2)_5]^{2+}$, the values increase to k_{ex}^{298} = 1.2 × 10^5 s^{-1} and $\Delta V^{\ddagger}$ = +7.0 cm^3 mol^{-1}. Hydrolysis causes lengthening of $\langle Fe^{III}-OH_2\rangle$ bonds because the overall charge of the complex is reduced from +3 to +2 and protons interconvert the bound hydroxyl to a bound water at rates much more rapid than the water exchanges. Thus, there is a correlation between complex lability and $\Delta V^{\ddagger}$ in these cases.

A conspicuous exception is the $[Fe(EDDS)(H_2O)]^-$ complex [Table 1], which has $\Delta V^{\ddagger}$ = −14.4 cm^3 mol^{-1}, near the extreme limit of pathways that would be considered associative, or **A**. These are uncommon (refs 29 and 30) and the authors interpreted their result to indicate a profound change in coordination and also cautioned about breakdown of the complex at temperatures greater than 310 K. The complex has no bound waters in the solid state but the authors suggest that one bonded carboxylate group releases in solution to allow a water to bind. This change in structure facilitates associative

dx.doi.org/10.1021/ic300370q | Inorg. Chem. 2012, 51, 6731−6738

ligand exchanges, the authors argue.[34] Other six-coordinated iron complexes in Table 1 do not exhibit evidence for an associative pathway and this may be due to the large bulky ligand around the iron center that blocks addition of a seventh coordinating atom.

Cause of the covariation in fitted $\Delta H^{\ddagger}$ and $\Delta S^{\ddagger}$ cannot be attributed to contribution of enthalpy from a deprotonation reaction because it has an endothermic enthalpy of reaction (ΔH_{rxn} = 63.3 (±5.9) kJ mol^{-1}, Supporting Information) as one expects for separation of charge. This enthalpy would *add* to the barrier for ligand exchange if a less-reactive complex dominated at high pH, not subtract. We do not understand and cannot evaluate the striking compensatory relation between fitted values of $\Delta H^{\ddagger}$ and $\Delta S^{\ddagger}$ indicates ligand dynamics at pH ~ pK_{a1}.

We are aware that small concentrations of highly reactive, and undetected, monomer ions could invalidate our interpretation. All studies that employ the Swift−Connick method for establishing rates are so vulnerable because only changes in the line width of the bulk-water peak are measured. However, we see no evidence for dissociation of the molecule. Furthermore, increased reactivity of the conjugate base of the $[Fe_4(OH)_2(hpdta)_2(H_2O)_4]^0(aq)$ molecule probably is not affecting the results, unlike the case for the octahedral monomer ions, such as $[Fe(OH_2)_6]^{3+}(aq)$. Upon deprotonation of $[Fe(OH_2)_6]^{3+}(aq)$ to form $[FeOH(OH_2)_5]^{2+}(aq)$, rates of exchange of bound waters increase by ~10^2 times[8] and the $\Delta V^{\ddagger}$ values indicate a clear change in reaction mechanism toward a more dissociative pathway ($\mathbf{I_d}$). This chemistry is in sharp contrast with the case here, where reactivity decreases as pH approaches pK_{a1} and there is no measurable change in $\Delta V^{\ddagger}$ values.

It is not surprising that the conjugate base would be less reactive than $[Fe_4(OH)_2(hpdta)_2(H_2O)_4]^0(aq)$ molecule. In $[Fe(OH_2)_6]^{3+}(aq)$ and $[FeOH(OH_2)_5]^{2+}(aq)$, bound waters and bound hydroxide are close packed and interconvert rapidly by simple proton shuttling among nearby functional groups. The reduced charge as $[Fe(OH_2)_6]^{3+}(aq)$ converts to $[FeOH(OH_2)_5]^{2+}(aq)$ is also averaged over a relatively small volume of ~111 cm^3/mol (calculated using density functional theory at the B3LYP/dgdzvp/PCM level of theory, this work). However, similar processes do not affect water-exchange rates in the $[Fe_4(OH)_2(hpdta)_2(H_2O)_4]^0(aq)$ molecule, where the bound waters remain fully protonated over the entire pH range of this study (pH < pK_{a1}) and the Brønsted reaction affects the bridging oxygen in the center of the molecule. Furthermore, the bound waters are separated from one another by ~5.2 Å and the molecule is five times larger than the aqua ion (~520 cm^3/mol; B3LYP/dgdzvp/PCM level of theory; this work). Thus, it is not unreasonable to expect that deprotonation of the $[Fe_4(OH)_2(hpdta)_2(H_2O)_4]^0(aq)$ molecule would reduce the lability of bound waters.

CONCLUSIONS

Rates of water exchange on the $[Fe_4(OH)_2(hpdta)_2(H_2O)_4]^0(aq)$ molecule fall into the same range as for other Fe(III) molecules, suggesting that rates of ligand exchange at bound-water sites are not dramatically affected by subtle details of structure. Rates trend with $\langle Fe^{III}-OH_2\rangle$ bond lengths and this variable alone seems to capture variations in lability due to small changes in average charge of the complex and structure, to at least within the small set of structures studied. A similar conclusion was derived from rare-events simulation of mineral-bound waters and experiments on aluminum aqueous complexes.[7] Wang et al.[7] used these data to show a correlation with bond lengths and predicted surprisingly rapid rates in most cases. Unless there were steric hindrances to exchange, the logarithm of rates scaled well with $\langle Al-OH_2\rangle$ bond length and were many orders of magnitude more rapid than for the fully protonated monomer ion, $[Al(OH_2)_6]^{3+}$.

The data in Figure 7 suggests that rates of exchange of bound and bulk waters are probably in the 10^6-10^7 s^{-1} scale at high-spin iron-oxide surface sites. The rates could be dramatically affected by steric influence and changes in electronic structure, of course, such as by partial reduction of the metal centers. If electron exchange between metal sites has a low barrier energy, the rates of exchange of all surface-bound waters will be dramatically affected by injection of an electron (ref 35 for an example) into the extended structure.

ASSOCIATED CONTENT

Supporting Information

Additional information as noted in the text. This material is available free of charge via the Internet at http://pubs.acs.org.

AUTHOR INFORMATION

Corresponding Author

*E-mail: whcasey@ucdavis.edu.

Notes

The authors declare no competing financial interest.

ACKNOWLEDGMENTS

This manuscript benefited considerably from comments by particularly perceptive referees. Support for this research was via the National Science Foundation via EAR-0814242 to WHC. CAO thanks the Australian Research Council for a QEII Discovery project grant (DP110105530) and work by SJH was performed under the auspices of the U.S. Department of Energy by Lawrence Livermore National Laboratory under Contract W-7405-Eng-48 and Contract DE-AC52-07NA27344. Training cost for AFP were covered as part of the Materials Science of Actinides, an Energy Frontier Research Center funded by the U.S. Department of Energy, Office of Science, Office of Basic Energy Sciences under Award Number DE-SC0001089. The authors thank Mr. Chris Colla for help with the figures and Prof. Leone Spiccia for advice.

REFERENCES

(1) Balogh, E.; Todea, A. M.; Muller, A.; Casey, W. H. *Inorg. Chem.* **2007**, *46* (17), 7087−7092.
(2) Schmitt, W.; Anson, C. E.; Sessoli, R.; van Veen, M.; Powell, A. K. *J. Inorg. Biochem.* **2002**, *91* (1), 173−189.
(3) Grant, M.; Jordan, R. B. *Inorg. Chem.* **1981**, *20* (1), 55−60.
(4) Mizuno, M.; Funahashi, S.; Nakasuka, N.; Tanaka, M. *Inorg. Chem.* **1991**, *30* (7), 1550−1553.
(5) Kumar, P.; Kumar, M.; Ramanathan, A.; Tsujimura, M. *Environmental Geochemistry and Health* **2010**, *32* (2), 129−146.
(6) Rustad, J. R. *Adv. Inorg. Chem.* **2010**, *62*, 391−436.
(7) Wang, J.; Rustad, J. R.; Casey, W. H. *Inorg. Chem.* **2007**, *46* (8), 2962−2964.
(8) Swaddle, T. W.; Merbach, A. E. *Inorg. Chem.* **1981**, *20* (12), 4212−4216.
(9) Schneppensieper, T.; Zahl, A.; van Eldik, R. *Angew. Chem., Int. Ed.* **2001**, *40* (9), 1678−1680.
(10) Ostrich, I. J.; Liu, G.; Dodgen, H. W.; Hunt, J. P. *Inorg. Chem.* **1980**, *19* (3), 619−621.

(11) Ako, A. M.; Waldmann, O.; Mereacre, V.; Kloewer, F.; Hewitt, I. J.; Anson, C. E.; Guedel, H. U.; Powell, A. K. *Inorg. Chem.* **2007**, *46* (3), 756−766.
(12) Schmitt, W.; Hill, J. P.; Juanico, M. P.; Caneschi, A.; Costantino, F.; Anson, C. E.; Powell, A. K. *Angew. Chem., Int. Ed.* **2005**, *44* (27), 4187−4192.
(13) Murugesu, M.; Clerac, R.; Wernsdorfer, W.; Anson, C. E.; Powell, A. K. *Angew. Chem., Int. Ed.* **2005**, *44* (41), 6678−6682.
(14) Powell, G., W.; Lancashire, H., N.; Brechin, E., K.; Collison, D.; Heath, S., L.; Mallah, T.; Wernsdorfer, W. *Angew. Chem., Int. Ed.* **2004**, *43* (43), 5772−5.
(15) Schmitt, W.; Anson, C. E.; Pilawa, B.; Powell, A. K. *Z. Anorg. Allg. Chem.* **2002**, *628* (11), 2443−2457.
(16) Schmitt, W.; Murugesu, M.; Goodwin, J. C.; Hill, J. P.; Mandel, A.; Bhalla, R.; Anson, C. E.; Heath, S. L.; Powell, A. K. *Polyhedron* **2001**, *20* (11−14), 1687−1697.
(17) Panasci, A. F.; McAlpin, J. G.; Ohlin, C. A.; Christensen, S.; Fettinger, J. C.; Britt, R. D.; Rustad, J. R.; Casey, W. H. *Geochim. Cosmochim. Acta* **2012**, *78* (1), 18−27.
(18) Catalano, J. G.; Fenter, P.; Park, C. *Geochim. Cosmochim. Acta* **2009**, *73* (8), 2242−2251.
(19) Schmitt, W.; Jordan, P. A.; Henderson, R. K.; Moore, G. R.; Anson, C. E.; Powell, A. K. *Coord. Chem. Rev.* **2002**, *228* (2), 115−126.
(20) Schmitt, W.; Anson, C. E.; Pilawa, B.; Powell, A. K. *Z. Anorg. Allg. Chem.* **2002**, *628* (11), 2443−2457.
(21) Ballard, L.; Reiner, C.; Jonas, J. *J. Magn. Reson., Ser. A* **1996**, *123* (1), 81−86.
(22) Swift, T. J.; Connick, R. E. *J. Chem. Phys.* **1962**, *37*, 307−20.
(23) Harley, S. J.; Ohlin, C. A.; Casey, W. H. *Geochim. Cosmochim. Acta* **2011**, *75*, 3711−3725.
(24) Frans, S. D.; Harris, J. M. *Anal. Chem.* **1984**, *56*, 466−470.
(25) Baes, C. F.; Mesmer, R. E. *The Hydrolysis of Cations*; Wiley: New York, 1976.
(26) Ohlin, C. A.; Villa, E. M.; Rustad, J., R.; Casey, W. H. *Nat. Mater.* **2010**, *9*, 11−19.
(27) Richens, D. *Comments on Inorganic Chemistry* **2005**, *26* (5−6), 217−232.
(28) Gorun, S. M.; Lippard, S. J. *Inorg. Chem.* **1991**, *30*, 1625−1630.
(29) Richens, D. T. *The Chemistry of Aqua Ions*. John Wiley: New York, 1997; p 592 pp.
(30) Helm, L.; Merbach, A. E. *Chem. Rev.* **2005**, *105* (6), 1923−1959.
(31) Swaddle, T. W. *Inorg. Chem.* **1980**, *19* (10), 3203−3205.
(32) Swaddle, T. W. *Comments on Inorganic Chemistry* **1991**, *12* (4), 237−58.
(33) Hubbard, C. D.; Van Eldik, R. *Inorg. Chim. Acta* **2010**, *363*, 2357−2374.
(34) Schneppensieper, T.; Seibig, S.; Zahl, A.; Tregloan, P.; van Eldik, R. *Inorg. Chem.* **2001**, *40* (15), 3670−3676.
(35) Ducommun, Y.; Newman, K. E.; Merbach, A. E. *Inorg. Chem.* **1980**, *19*, 3696−3703.
(36) Maigut, J.; Meier, R.; Zahl, A.; van Eldik, R. *Inorg. Chem.* **2007**, *46* (13), 5361−5371.